Study of Capillary Filling Dynamics in a Microchannel

A project report submitted in the partial fulfillment of the requirements for the degree of

B. Tech

(Mechanical Engineering)

By

Manisha swain

Roll no- 107MEo36

Under the supervision of

Dr Ashok ku. Satapathy

Associate Professor

Department of Mechanical Engineering

NIT, Rourkela

Department of Mechanical Engineering

National Institute of Technology, Rourkela

Study of Capillary Filling Dynamics in a Microchannel

A project report submitted in the partial fulfillment of the requirements for the degree of

B. Tech

(Mechanical Engineering)

By

Manisha swain

Roll no- 107MEo36

Under the supervision of

Dr Ashok ku. Satapathy

Associate Professor

Department of Mechanical Engineering

NIT, Rourkela

Department of Mechanical Engineering

National Institute of Technology, Rourkela

National Institute of Technology
Rourkela

CERTIFICATE

This is to certify that the work in this thesis entitled "**Study of Capillary filling dynamics in a micro channel"** by **Manisha Swain,** has been carried out under my supervision in partial fulfillment of the requirements for the degree of **Bachelor of Technology** in ***Mechanical Engineering*** during session 2010- 2011 in the Department of Mechanical Engineering, National Institute of Technology, Rourkela.

To the best of my knowledge, this work has not been submitted to any other University/Institute for the award of any degree or diploma.

Dr. Ashok ku. Satapathy

(Supervisor)

Associate Professor

Department of Mechanical Engineering

National Institute of Technology Rourkela – 769008

ACKNOWLEDGEMENT

I would like to express my deep sense of gratitude and respect to my supervisor Prof. **ASHOK SATAPATHY** for his excellent guidance, valuable suggestions and endless support.

I am also thankful to **Prof. R. K. SAHOO**, H.O.D, Department of Mechanical Engineering, N.I.T Rourkela for his constant support and encouragement.

Last, but not the least I extend my sincere thanks to other faculty members of the Department of Mechanical Engineering, NIT Rourkela, for their valuable advice in every stage for successful completion of this project report.

Manisha Swain

Roll no-107ME036

Mechanical Engineering Department

National Institute of Technology, Rourkela

ABSTRACT

Capillary filling dynamics in a micro channel and different aspects of this type of flow has remained a long-acting problem in the last decade considering its numerous applications in various fields. In this study, an attempt has been made to study the influence of certain parameters on the equilibrium height attained by the liquid in the micro channel. Lucas Washburn equation has been modified using the concept of phase change and vapour recoil and also accommodating the entrance effects in terms of added mass. The formulated governing equation was used to study the effect of parameters such as: phase change, aspect ratio and properties of the liquid numerically using MATLAB. Two different liquids water and ether has been used in the analysis. It was found that phase change by evaporation resulted in lowering of liquid rise. Also the oscillations in water were found to be damped more than those in ether. It was also revealed that liquid rise increased with increasing aspect ratio and with increase in aspect ratio, the change in equilibrium height gradually decreased. The effect of contact angle on the flow characteristics was also studied.

CONTENTS

CHAPTER 1

INTRODUCTION

Microfluidics deals with the behavior of fluids in the sub millimeter range and its study requires different approach from the conventional ones used for macrofluidics though fundamental physics for both remains the same. Thus the differences and deviations between microfluidics and macrofluidics in various aspects have been studied widely. It is a diverse field intersecting engineering, physics, chemistry, micro-technology and biotechnology, with applications to the design of systems in which small volumes of fluids will be used. Numerous applications of microfluidic devices in diverse fields like biomedical science, MEMS devices, lab on a chip technology, micro scale heat exchanger and micro heat pipes has made the study of the subject both relevant as well as significant.

Since the introduction of micro channel fluid flow as an effective means of cooling of electronic equipments, both experimental investigations and numerical predictions have been undertaken to study the microscale transport phenomena. Deviations of the results obtained by theoretical simulations from the experimental observations have resulted in modification of existing theories. Interpretation of findings and subsequent changes have led to a better understanding of various phenomena occurring in micro channel flow and of different factors affecting the flow characteristics.

The behavior of fluids at the microscale can differ from 'macrofluidic' behavior as factors such as surface tension, energy dissipation, and fluidic resistance start to dominate the

system. Microfluidics studies how these behaviors change, and how they can be worked around, or exploited for new uses.

Advances in microfluidics technology are revolutionizing molecular biology procedures for enzymatic analysis (e.g., glucose and lactate assays), DNA analysis (e.g., polymerase chain reaction and high-throughput sequencing), and proteomics. The basic idea of microfluidic biochips is to integrate assay operations such as detection, as well as sample pre-treatment and sample preparation on one chip. An emerging application area for biochips is clinical pathology, especially the immediate point-of-care diagnosis of diseases. In addition, microfluidics-based devices, capable of continuous sampling and real-time testing of air/water samples for biochemical toxins and other dangerous pathogens, can serve as an always-on "bio-smoke alarm" for early warning. Another application of microfluidics is micro heat pipe. Understanding the two-phase flow behavior and thin film evaporation in microchannels is the key to developing microchannel heat pipes for high-power microprocessors.

In this study, the capillary flow phenomena in microchannels was theoretically formulated using the Lucas Washburn equation. Lucas Washburn equation has been used by several investigators who have compared the numerical results obtained to the experimental observation. However in some cases deviations have been noticed. Here we have included the concept of added mass and vapour recoil and theoretically formulated the Lucas Washburn equation. Added mass accounts for the entrance effects whereas vapour recoil gives the thrust experienced by the rising liquid during phase change (evaporation /condensation). Numerical analysis was done using MATLAB to

study the flow characteristics of two different fluids water and ether. The liquids were chosen keeping in mind the large variation in different properties so that the analysis will involve a wide range of values of different properties like density, vapour density and viscosity.

A long vertical capillary of width w and height h was considered which is brought in contact with a large reservoir of a liquid with density ρ and viscosity μ. The liquid was kept at a constant temperature, which may be above (or below) a reference saturation temperature of the vapor within the capillary by the value ΔT depending on which evaporation (or condensation) takes place.

The objective was to study the effect of the various flow parameters on the time course of displacement of fluid and equilibrium height attained. The different parameters studied include phase change consideration, temperature differences across the interface, static and dynamic contact angle, different aspect ratio (w/H) of the rectangular micro channel. An attempt was made to study the damping of oscillations in the two different fluids used.

CHAPTER 2

LITERATURE SURVEY

Peng et al. [25] experimentally studied the flow of water in rectangular micro channels with hydraulic diameters in the range of 0.13 to 0.37 mm and aspect ratios from 0.3 to 1.0. The channels were machined on stainless steel substrate. According to the results the flow transition occurs at Reynolds number 200–700 which is very different from the conventional results. The transitional Reynolds number is observed to diminish with reductions in microchannel dimensions.

Pfahler et al. [26, 27] investigated the flow characteristics of different fluids in microchannels including nitrogen and helium gases, isopropyl liquid and silicone oil. The microchannels were fabricated on silicon wafer by etching method. It was observed that for the smaller microchannels, the test results deviated from the prediction of conventional theories.

Mohiuddin Mala et al. [28] measured pressure gradients of water flow in microtubes with diameters in the range of 0.05 to 0.254 mm and the results indicated that for the larger microtubes with inner diameter above 150 μm, the experimental results roughly matched the prediction of conventional theories. For the smaller microtubes, larger deviations were observed. With increase in Re, the differences between the experimental findings and the conventional theory predictions increased. This increasing difference was accounted for early transition from laminar to turbulent flow.

Stanley [29] carried out some experiments of the single-phase and two phase liquid flow in microchannels machined on aluminum plate. The hydraulic diameters of the microchannels varied from 0.056 to 0.26 mm. Based on the experimental data, for water flow, it was stated that no transition occurred at any size of channels at any Reynolds numbers, from 2 to 10000.

Gas liquid two phase flow regimes were studied by different investigators and the various regimes as observed experimentally in case of microchannels were different from that of macroscale predictions.

Guy Ramon and Alexander Oron extended the Lucas-Washburn equation to account for the phase change and interfacial mass transfer due to phase change – evaporation or condensation. The augmented equation developed contained contributions related to mass loss/gain and also an additional effective force, vapor recoil which occurs as a result of the velocity jump at the interface. Several properties of the system behavior were altered due to the phase change.

A number of studies were conducted in straight- walled ducts having a variety of cross sectional shapes. Ducts having unusual cross-sections or stream wise variations in cross section were considered. Among different geometries that were investigated, circular, trapezoidal and triangular cross sections were given more importance than others.

A generalized model for heat, mass transport and particle dynamics near an evaporating meniscus was proposed by PAN and WANG. The evaporation on the meniscus, vapor

diffusion in vapor/air domain, buoyant convection and particle dynamics were coupled together.

Deryagin et al [1] and [2] demonstrated liquid pressure reduction in the thin-film region due to disjoining pressure. Potash and Wayner [3] concluded that the variation of disjoining pressure and capillary pressure along the meniscus provides the necessary pressure gradient for liquid supply into the thin-film region. Wayner et al [4] discussed the effects of disjoining pressure on liquid supply as well as its role in suppressing evaporation. An augmented Young–Laplace equation was obtained for force balance on the thin film by introduction of a disjoining pressure .Schonberg et al. [5] investigated the thin film by ignoring Pc. Hallinan et al.[6] and DasGupta et al. [7] developed a fourth-order ordinary differential equation for solving the augmented Young–Laplace equation and obtained the thickness profile of the extended meniscus. The influence of superheat on the thin-film profile was discussed. Park et al. [8] proposed a mathematical model which included the vapor region and a slip boundary condition. It was concluded that the pressure gradient in the vapor region significantly affected the thin-film profile. Wee [9] discussed the effects of liquid polarity, slip boundary and thermo capillary effects on the thin-film profile. The polarity effect was found to elongate the transition region while suppressing evaporation. Recently, binary liquids [10] have been found to induce a distillation-driven capillary stress to counteract the thermo capillary stress, leading to an elongation in thin-film length. Atomistic simulations by Freund [11] showed that the thermal resistance at the solid–liquid interface is significant in very thin films. The menisci in more complex geometries have also been studied. Stephan and Busse [12] calculated the heat and mass transfer in the micro-region and then combined the solution with the macroscopic meniscus within

open grooves. Xu and Carey [13] conducted a combined analytical and experimental investigation on the liquid flow in V grooves and emphasized the importance of disjoining pressure on the overall heat transfer. Ma and Peterson [14] proposed a mathematical model for the evaporation heat transfer coefficient and temperature variation along the axial direction of a groove, which led to a better understanding of the axial heat transfer coefficient and temperature distribution on grooved surfaces. Morris [15] suggested a universal relationship between heat flow, contact angle, interface curvature, superheat and material properties, which can be extended to different geometries. Recently, thin-film evaporation in a microchannel was studied [16].

CHAPTER 3

THEORY

One of the characteristic features of microfluidics is the dominance of surface effects due to the large surface to bulk ratio on the micrometer scale. A prominent class of surface effects is known as capillary effects particularly strong in microchannels having bore diameters equal to or less than about 50 μm.

The capillary effects can be understood by studying Gibbs free energy G, the energy of systems where the thermodynamic control parameters are pressure p, temperature T, and particle number N. In particular we shall be interested in equilibrium or quasi-equilibrium situations, where the Gibbs free energy is at a minimum.

Surface Tension:

Surface tension is a property that relates to the surface or interfaces and depends on the state of the substance on both sides of the interface. The surface tension of an interface is defined as the Gibbs free energy per area for fixed pressure and temperature,

$$\Upsilon = \left(\frac{\partial G}{\partial A} \right)_{p,T} \tag{1}$$

A molecule in the bulk forms chemical bonds with the neighboring thus gaining a certain amount of binding energy. A molecule at the surface cannot form as many bonds since there are almost no molecules in the gas. This lack of chemical bonds results in a higher energy for the surface molecules. This is exactly the surface tension: it costs energy to form a surface. Using this model it is easy to estimate the order of magnitude of surface tension for a liquid-gas interface.

Surface tension can also be interpreted as a force per length having the unit N/m =J/m². This can be seen by considering a flat rectangular surface of length L and width w. If we keep the width constant while stretching the surface the amount ΔL from L to $L + \Delta L$, an external force F must act to supply the work $\Delta G = F\,\Delta L$ necessary for creating the new surface area ($w\,\Delta L$) containing the energy $\Delta G = \gamma\, w\,\Delta L$,

$$\frac{F}{w} = \frac{1}{w}\frac{\Delta G}{\Delta L} = \frac{1}{w}\frac{\Upsilon w \Delta L}{\Delta L} = \Upsilon \qquad (2)$$

The Young Laplace pressure across curved interfaces:

An important consequence of a non-zero surface tension is the presence of the so-called Young Laplace pressure drop (Δp_{surf}) across a curved interface in thermodynamic equilibrium.

If we disregard any influence of gravity there will only be two contributions to the change ΔG of the free energy of the system: an increase in surface energy G_{surf} due to an increased area, and a decrease in pressure-volume energy G_{pV} due to the increase in volume. It is important to note the sign convention used here: the pressure is highest in the convex medium, i.e., the medium in which the centre of curvature lies.

Contact angle:

Another fundamental concept in the theory of surface effects in microfluidics is the contact angle that appears at the contact line between three different phases, typically the solid wall of a channel and two immiscible fluids inside that channel. The two concepts, contact angle and surface tension, allow for understanding the capillary forces that act on two-fluid flows inside microchannels in lab-on-a-chip systems.

Definition of the contact angle:

The contact angle θ is defined as the angle between the solid-liquid and the liquid-gas interface at the contact line where three immiscible phases meet, as illustrated in Fig. 3.1 (a).

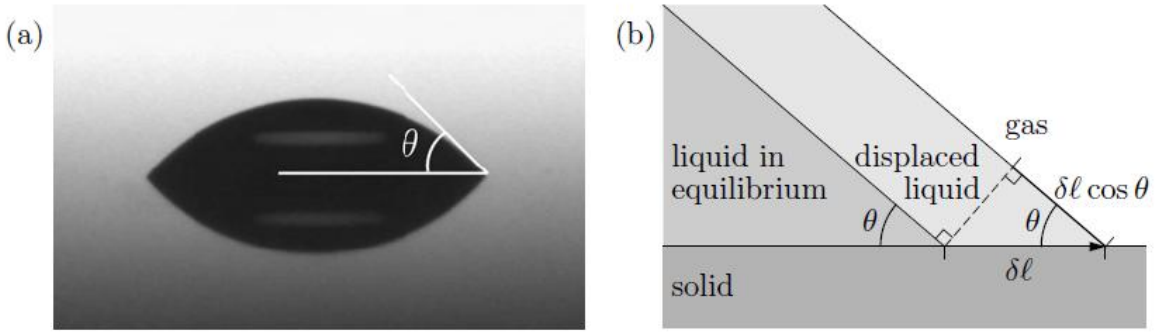

[Figure 3.1 (a): The contact angle θ is defined as the angle between the solid-liquid and the liquid-gas interface at the contact line.

(b) A sketch of the small displacement δl of the contact line away from the equilibrium position. The change of the interface areas are proportional to $+\delta l$, $+\ \delta l \cos\theta$, and $-\delta l$ for the solid-liquid, liquid-gas, and solid-gas interface, respectively.]

In equilibrium θ is determined by the three surface tensions γ_{sl}, γ_{lg}, and γ_{sg} for the solid-liquid, liquid-gas and solid-gas interfaces by Young's equation to be discussed in the following subsection. Whereas the contact angle is well-defined in equilibrium it turns out to depend in a complicated way on the dynamical state of a moving contact line. One can for example observe that the contact angle at the advancing edge of a moving liquid drop on a substrate is different from that at the receding edge.

Young's equation; surface tensions and contact angle:

To derive an expression for the contact angle in equilibrium we again use the free energy minimum condition. We consider the system sketched in Fig. 3.1(b), where in equilibrium a flat interface between a liquid and a gas forms the angle θ with the surface of a solid substrate. Imagine now that the liquid-gas interface is tilted an infinitesimal angle around an axis parallel to the contact line and placed far away from the substrate interface. As a result the contact line is moved the distance δl while keeping the contact angle θ. To order δl the only change in free energy comes from the changes in interface areas near the contact line. It is easy to see from Fig. 3.1(b) that the changes of the interface areas are proportional to $+\delta l$, $+\delta l \cos\theta$, and $-\delta l$ for the solid-liquid, liquid-gas, and solid-gas interface, respectively. The energy balance at the interface gives,

$$\cos\theta = \frac{\Upsilon_{sg} - \Upsilon_{sl}}{\Upsilon_{lg}} \qquad (3)$$

Capillary rise:

In the previous discussion gravity was neglected, an approximation that turns out to be very good in many cases for various microfluidic systems. The equilibrium shape of any liquid will be determined by minimizing the free energy G consisting of the surface energy and the gravitational potential energy of the bulk, with constant volume constraint. The equilibrium shape for a free liquid drop in zero gravity is a sphere, since the sphere has the minimal area for a given volume. Gravity does not influence the shape of free water-air interfaces in microfluidic systems of sizes a well below 1 mm. This insight can be used to analyze the so-called capillary rise that happens in narrow, vertically standing

microchannels. The shape problem is governed by a characteristic length, the so-called capillary length l_{cap},

$$l_{cap} = \sqrt{\frac{\Upsilon}{\rho g}} \tag{4}$$

Capillary rise can be observed as sketched in Fig. 3.2(b) by dipping one end of a narrow open-ended tube into some liquid. The liquid will rise inside the tube until it reaches equilibrium at some height H above the zero level z = 0 defined as the flat liquid level far away from the tube. The task is to determine H.

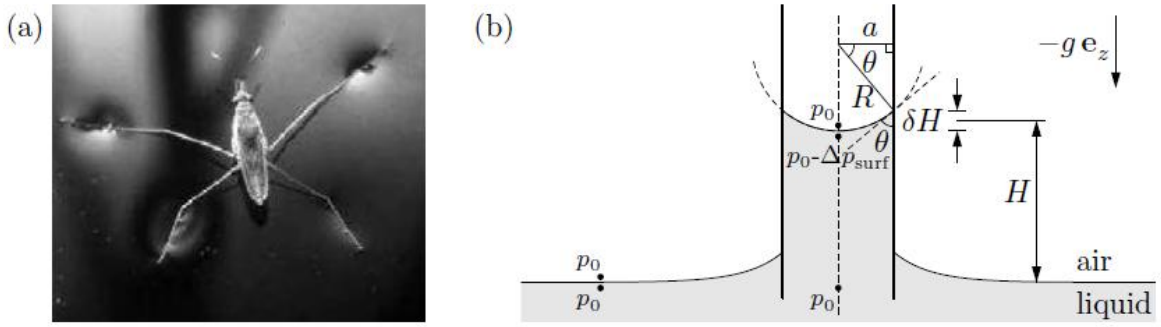

Figure 3.2(a): The importance of surface tension for microsystems illustrated by an insect able to walk on water. The gravitational force is balanced by the surface tension of the water-air interface. (b) Capillary rise in a vertically standing cylindrical microchannel.

Systems with contact angles $\theta < 90°$ are called hydrophilic (water loving) while those with $\theta > 90°$ are called hydrophobic (water fearing).

Capillary rise height:

For simplicity we consider a vertically placed micro-tube with a circular cross section of radius $a << l_{cap}$. The contact angle of the tube-liquid-air system is denoted μ and the

surface tension of the liquid-air interface is called °. Because $a \ll l_{cap}$ and because the tube is circular the liquid-air surface of minimal energy inside the tube will be spherical. Thus the two radii of curvature are identical, and from the geometry of Fig. 3.2(b) we find,

R1 = R2 = R = a/cos θ

Because the liquid-air interface is curved, a Young Laplace pressure drop Δp_{surf} will be present across it. Balancing the hydrostatic pressure with the Young Laplace pressure drop at the interface the capillary rise height is found as follows.

$$H = \frac{2\gamma}{\rho g a} \cos\theta \qquad (5)$$

Concept of dynamic contact angle:-

The capillary effect within the microchannel essentially implies that a fluid-fluid interface and fluid-solid interface interact to form a tri-junction. In order to model moving contact lines appropriately one needs to first qualitatively assess the physical phenomena influencing the capillarity. In a physical sense, this departure of the contact angle from its static value is because of the viscous bending of the interface at the contact lines.

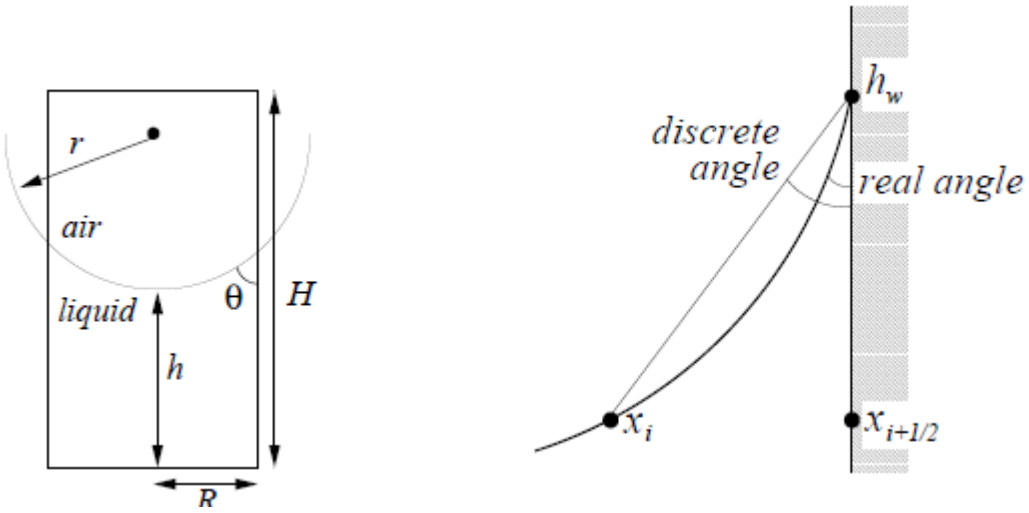

Fig. 3.3: illustration of dynamic contact angle

The apparent dynamic contact angle θ_d that the liquid forms with the solid surface is closely described by a universal scaling relationship at low speeds, known as Tanner's law:

$$\text{Ca} \sim \theta^{\frac{1}{3}} \qquad (6)$$

Where $Ca = \frac{\mu u}{\gamma}$, μ= viscosity and u= velocity of contact line

*****

CHAPTER 4

THEORITICAL FORMULATION

When a droplet of fluid comes in contact with a micro capillary channel, surface tension draws it into the channel and induces the fluid into motion. This is typical to many biomicrofluidic applications (for example, in medical or dental applications) when blood droplets come in contact with artificially grafted micro fluidic channels. The effect of surface tension on the flow of blood is significant, especially in micro scale. The leading edge of the flowing blood is the triple point where the blood, the material surface, and a stationary gas or fluid meets. The movement of the triple point, i.e., the advancing front of the flow, is driven by surface tension, resisted by viscous shear stress, and balanced by the inertial force. The equation of motion describing the advancement of a liquid meniscus in a gas- filled capillary can be given by the Newton's second law:

$$\frac{d}{dt}(MV_c) = \sum F \qquad (7)$$

where M is the fluid mass being transported, Vc is the velocity of its center of mass and F = Fsurface tension + Fviscous+ Fgravity. Microchannel flows are typically characterized with low Bond Numbers (which are indicators of the ratio of gravity to surface tension force), and therefore the gravity force is neglected in this analysis.

For a micro channel of depth H and width w, with instantaneous axial length (averaged over the cross section) occupied by the fluid as l, the governing equation of fluid motion can be written as:

$$\frac{d}{dt}\left((M_a + \rho H w l)\frac{dl}{dt}\right) = P\sigma\cos\theta - F_D \qquad (8)$$

where ρ is density of the fluid, P is the wetted perimeter(P = 2(w + H)), σ is the surface tension coefficient, θ is the contact angle, and F_D is the viscous drag force. Physically, eqn. (8) represents the Newtonian equation of motion of the liquid column in the capillary. The first term in the right hand side of eqn. (8) represents the surface tension force and the second term represents a viscous drag force. The term M_a in eqn. (8) is a so-called added mass, which accounts for the mass of the fluid droplet on the verge of entering the micro capillary channel. This can be mathematically modeled by drawing analogy from potential flow of a circular cylindrical lumped fluid mass of radius rh, moving along the x-direction, where rh is hydraulic radius of the channel, given by:

$$r_h = \frac{2wH}{2(w+H)}, \quad \text{Added mass } M_a = \frac{\rho\pi H^2 w}{8}$$

Modeling of the overall viscous drag:

Entrance region and different flow regimes i.e. fully developed regime (which is characterized by a so-called Poiseuillean velocity profile) and so-called meniscus traction regime give rise to modified drag :-

$$\frac{dF_D}{dx} = \left[1 + f\left(\frac{x}{r_h}\right)\right]\frac{dF_D^*}{dx}$$

where $f\left(\frac{x}{r_h}\right) = a_0 + a_1\left(\frac{x}{r_h}\right) + a_2\left(\frac{x}{r_h}\right)^2 \qquad (9)$

On integrating:-

$$F_D = w r_h \left[\frac{\bar{x}_1}{r_h} + 2 f_1\left(\frac{\bar{x}_1}{r_h} \right) \right] \frac{dF_D^*}{dx} \qquad for \quad 0 \le \frac{\bar{x}_1}{r_h} \le 1.4$$
$$= w r_h \left[\frac{\bar{x}_1}{r_h} + 2 f_1\big|_{max} \right] \frac{dF_D^*}{dx} \qquad for \quad \frac{\bar{x}_1}{r_h} > 1.4 \tag{10}$$

Where

$$f_1\left(\frac{x}{r_h} \right) = \int_0^{X/r_h} f\left(\frac{x}{r_h} \right) d\left(\frac{x}{r_h} \right)$$

Hence

$$F_D = -\frac{12\mu w}{h} l \frac{dl}{dt} - f_1\left(\frac{\bar{x}_1}{r_h}\right) 12\mu w \frac{dl}{dt} \tag{11}$$

$$f_1\left(\frac{\bar{x}_1}{r_h} \right) = \begin{cases} 2.9665\left(\frac{\bar{x}_1}{r_h}\right) - 4.7344\left(\frac{\bar{x}_1}{r_h}\right)^2 + 2.6134\left(\frac{\bar{x}_1}{r_h}\right)^3 & for \quad \frac{\bar{x}_1}{r_h} \le 1.4 \\ 0.62 \quad for \quad \frac{\bar{x}_1}{r_h} > 1.4 \end{cases}$$

In case of phase change, another force comes into play. Normally, phase change at the interface creates large accelerations of the vapor due to a large disparity in liquid and vapor densities, and the backward reaction is known as vapor recoil. The pressure exerted by vapor recoil on the interface is directed into the liquid phase for both evaporation and condensation and Hickman found that vapor recoil can be very important in terms of the behavior of the gas–liquid interface where phase change takes place, especially under conditions of reduced pressure. This pressure is the result of the velocity jump which the vapor undergoes during evaporation/condensation. Since the phase change creates a density jump, a corresponding velocity jump is necessary for the

mass flux to be continuous at the interface. The kinematic boundary condition at the interface requires [21] that

$u = \left(\frac{dl}{dt} + \frac{j}{\rho} \right)$ where j is the interfacial mass flux due to evaporation/condensation. Hence the governing equation of fluid motion can be written as:-

$$\frac{d}{dt}\left((M_a + \rho Hwl)\left(\frac{dl}{dt} + \frac{j}{\rho} \right) \right) = P\sigma \cos\theta - F_D - \frac{j^2}{\rho_v} \qquad (12)$$

Where $F_D = -\frac{12\mu w}{h} l \left(\frac{dl}{dt} + \frac{j}{\rho} \right) - f_1(\frac{\overline{x}_1}{r_h}) 12\mu w \left(\frac{dl}{dt} + \frac{j}{\rho} \right)$

The resulting mass flux may be approximated using kinetic theory which in linearized form reads [21],[22],[23];

j=k*(tl-tv) where tl,tv denotes the temperature at the interface and the vapour respectively

$$k = \frac{\alpha \rho_v L}{T_v^{3/2}} \left(\frac{M_w}{2\pi R_g} \right)^{1/2} \qquad (13)$$

Here Rg is the universal gas constant, Mw is the molecular mass of the liquid, and α is the accommodation coefficient, taken here as unity.

Governing equation of the capillary filling in the rectangular microchannel:

Thus, the governing equation of the capillary filling in the rectangular microchannel with temperature difference across the interface is:

$$\frac{d^2 l}{dt^2} = \left(\mathrm{P}\sigma\cos\theta - \frac{dl}{dt}\left(\frac{12\mu_w l}{\mathrm{H}} + 12 f_1\left(\frac{\bar{x}_1}{rh}\right)\mu_w \right) - \frac{j}{\rho}\left(\frac{12\mu_w l}{\mathrm{H}} + 12 f_1\left(\frac{\bar{x}_1}{rh}\right)\mu_w \right) - \left(\frac{j^2}{\rho_v} w\mathrm{H} \right) - \rho \mathrm{H} w \left(\frac{dl}{dt} \right)^2 \right) \Bigg/ \left(\frac{\rho\pi \mathrm{H}^2 w}{8} + \rho \mathrm{H} w l \right)$$

(14)

The dynamic contact angle was modeled using Tanner's relationship:

$$\mathrm{Ca} \sim \theta^{\frac{1}{3}}$$

The dynamic contact angle was modified according to the varying Capillary number .

*****

CHAPTER 5

RESULTS AND DISCUSSION

The properties of two different fluids used for analysis is shown in the following table.

Table 1 (Properties of fluids used):

Properties	Water	Ether
Fluid density(ρ) (kg/m^3)	1000	70
Vapour density(ρ_v)(kg/m^3)	0.804	3.14
Surface tension coefficient(σ) (N/m)	0.072	0.016
Coefficient of viscosity(μ)	0.001	$2.23\times e^{-4}$
Static contact angle (θ) (with glass)	30	0
Latent heat of vaporization(L) (kJ/kg)	2360	377
Molecular weight (kg/mol)	0.018	0.074

The properties as given in the above table show that water has a higher density than ether whereas density of vapour of water is less than that of ether. Coefficient of viscosity for water exceeds significantly that of ether. There are differences in other properties also. The liquids chosen are expected to show variation in results. For the flow of water, we have considered a square micro channel of widh and height 0.05 mm whereas for ether a width of 0.5 μm and height 150 μm was used.

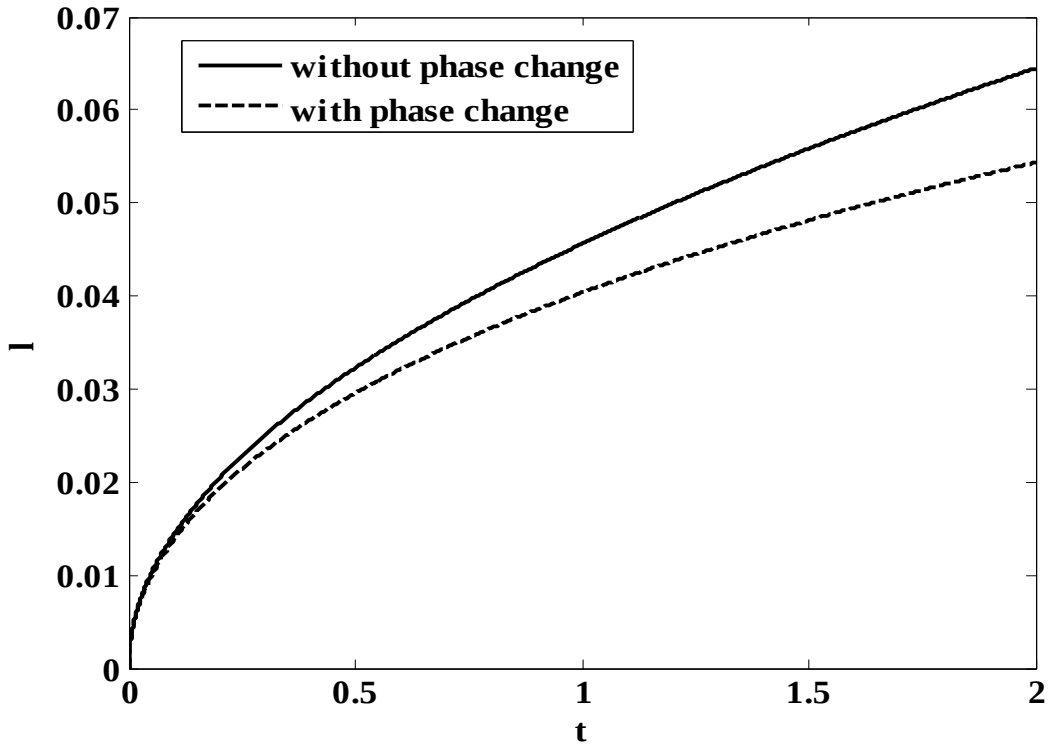

(Fig 5.1: Time course of displacement of fluid into the channel with phase change (evaporation) and without phase change consideration)

Fig-5.1 depicts advancement of the meniscus in the micro channel as a function of time. It can be observed that the displacement increases substantially if there is no phase change. The effect of the temperature difference which induces the phase change is apparent and decreases the displacement of the meniscus. This may be attributed to the fact that the vapor recoil term always induces a pressure in the negative direction, as seen in Eqn.(12) opposing the capillary flow, regardless of whether evaporation/condensation is present. In the presence of evaporation, $j>0$ and therefore the motion of the interface will be slower than with no phase change.

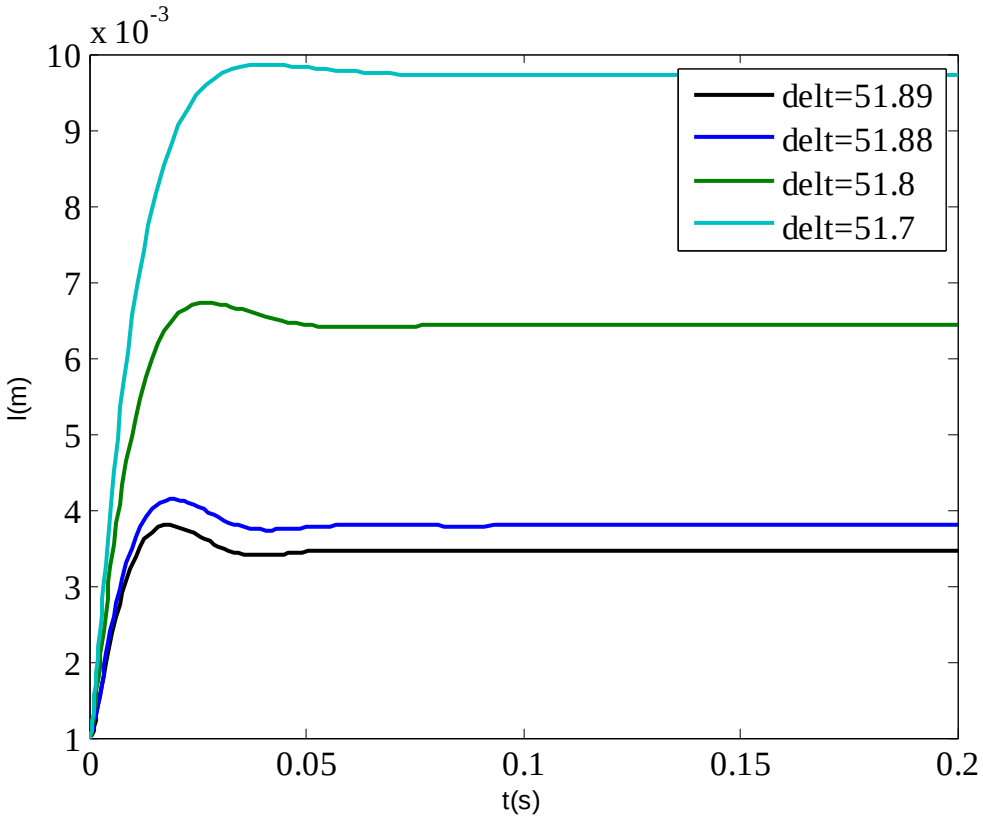

Fig 5.2**:** Time course of displacement of fluid into the channel for ether for different temperature differences across the interface.(delt =Tl-Tv; where Tl is the temperature of the interface and Tv is the temperature of the vapour.)

The effect of the temperature difference which induces the phase change is apparent and alters both the amplitude and frequency of the interfacial oscillations, when these are present. Fig-5.2 depicts that as the temperature difference across the interface increases, there is a decrease in the displacement of the meniscus. This indicates that due to increase in temperature difference, evaporation increases, thus the vapour recoil term (j>0) increases which opposes the capillary flow.

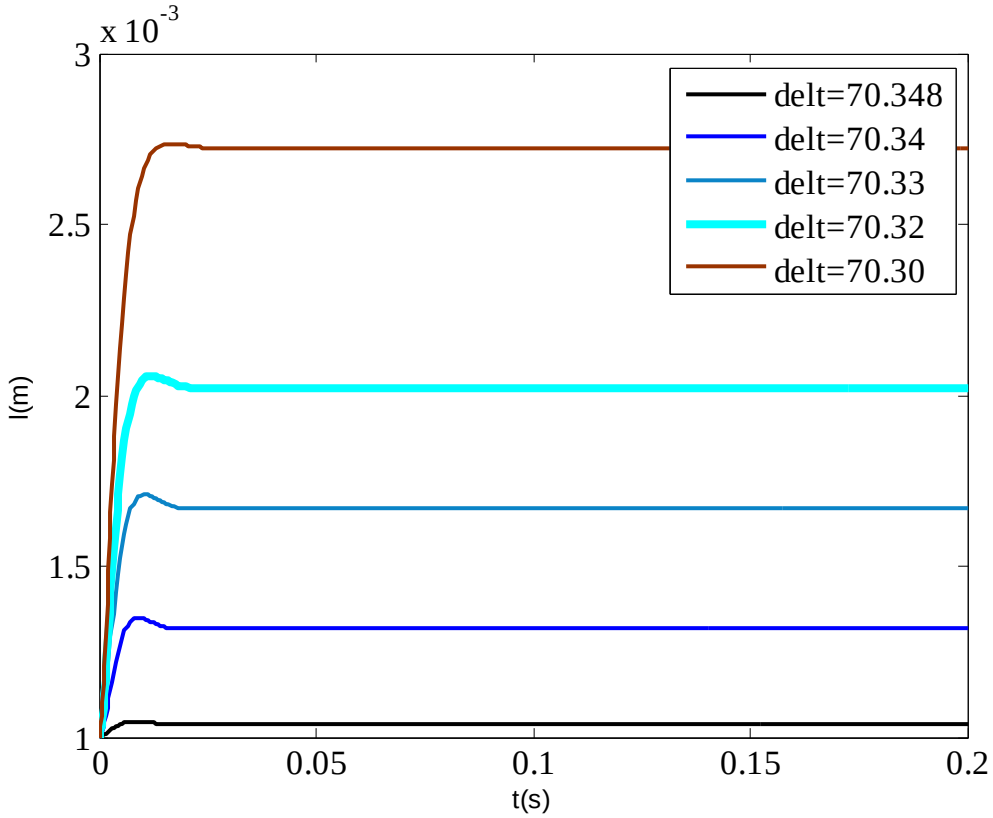

(Fig-5.3:-Time course of displacement of fluid into the channel for water for different temperature differences across the interface)

It is also seen that for a particular aspect ratio (w/H) ether oscillates faster than water possibly due to the lower surface tension .It is also seen that water oscillations decay faster than ether due to the stronger damping effect of the higher viscosity of water.

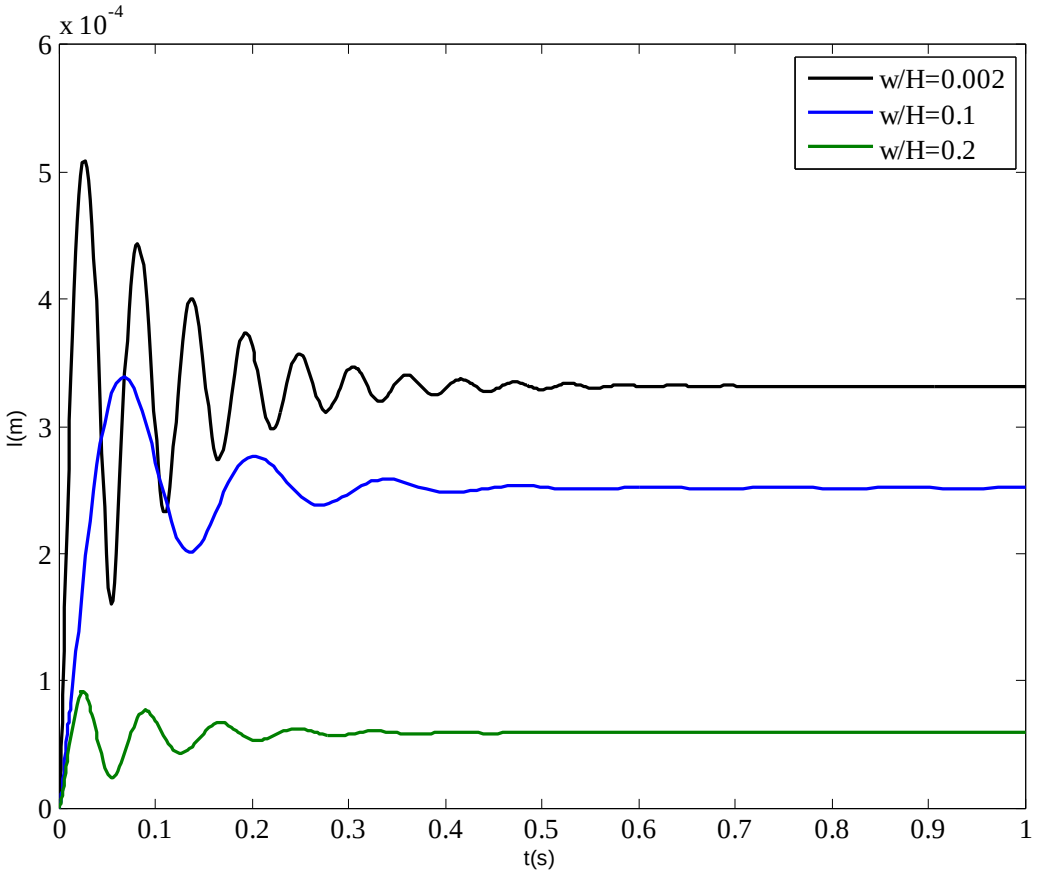

(Fig-5.4: Time course of displacement of fluid into the channel for ether for different aspect ratio (w/H) of the rectangular microchannel.)

It is observed in fig-5.4 that as the aspect ratio increases the amplitude of oscillations decreases and the oscillations also decay faster. The change in equilibrium height from 0.1 to 0.2 is more than that between 0.002 and 0.1. It is due to the fact that the constraining effect due to transverse side (side with smaller dimension) of the channel becomes less significant with increasing aspect ratio.

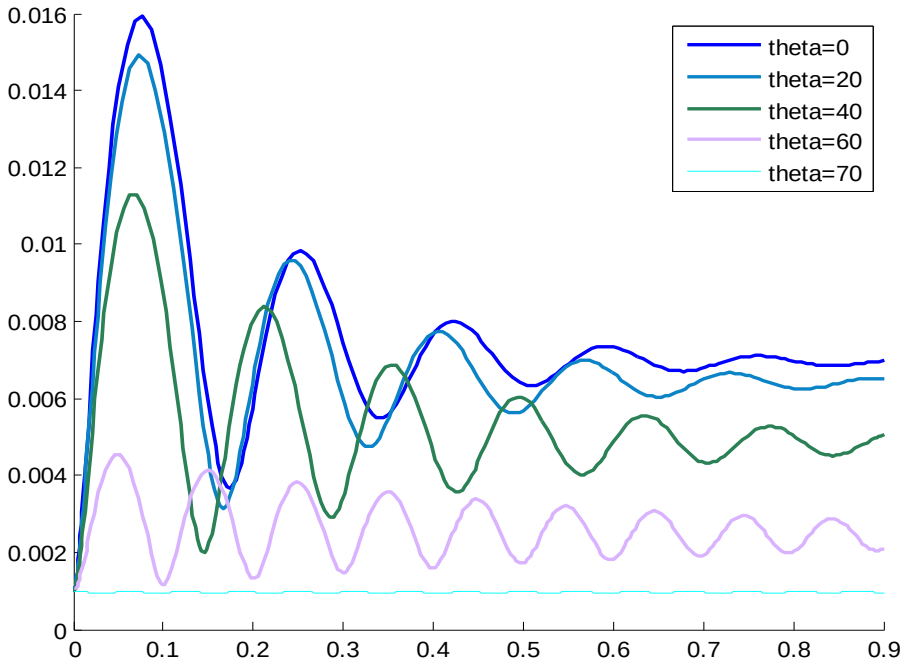

Fig-5.5: Effect of contact angle in the time course of fluid front flowing into a microchannel

Figure 5.5 shows the effect of the contact angle when fluid flows in a micro channel. A larger contact angle implies a lower height of liquid rise. And also the stability of flow increases with increasing contact angle. Higher amplitudes of oscillations are observed for lower contact angles.

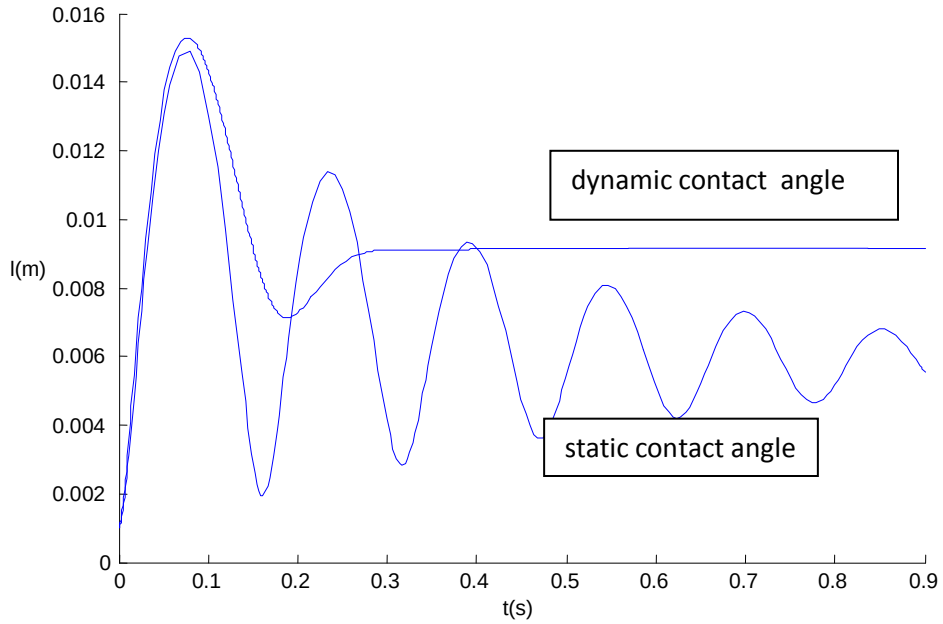

Fig-5.6: Time course of displacement of fluid into the micro channel for dynamic contact angle and static contact angle

Fig- 5.6 depicts the effect of a 'dynamic contact angle', as the fluid propagates inside the channel. Since velocity decreases as time increases, the Capillary number also decreases in accordance with the same, and consequently, the apparent contact angle also decreases. Since the surface tension force is proportional to the cosine of this contact angle, it increases progressively as the contact angle decreases, during in-flow process of the fluid. This, in turn, implies a stronger driving force against the viscous drag, leading to a larger displacement at a given instant of time.

CONCLUSIONS

The following conclusions were drawn from the results analyzed in the previous chapter.

- There is a decrease in displacement due to evaporation which is due to the increased vapor pressure on the liquid vapor interface. For a constant temperature difference, the decrease in equilibrium height increases with time.
- To achieve a particular equilibrium height during phase change, a higher value of temperature difference is required for water than for ether due to higher density of water and consequently high mass transfer.
- Oscillations decay faster in water due to its higher viscosity and higher damping coefficient than ether, other factors remaining constant.
- With increasing aspect ratio, equilibrium height increases. As aspect ratio goes on increasing, the effect of aspect ratio on the rise of liquid becomes gradually less significant. It can be predicted that after a certain limiting value of aspect ratio, the liquid height at equilibrium will become constant.
- Dynamic contact angle leads to a larger displacement at a given instant of time.

REFERENCES

[1] B.V. Deryagin, S.V. Nerpin and N.V. Churayev, Effect of film heat transfer upon evaporation of liquids from capillaries, Bull. R. I. L. E. M. 29 (1965), pp. 93–98.

[2] B.V. Deryagin, Modern state of the investigation of long-range surface forces, Langmuir 3 (1987) (5), pp. 601–606.

[3] M. Potash Jr. and P.C. Wayner Jr., Evaporation from a two-dimensional extended meniscus, Int. J. Heat Mass Transfer 15 (1972), pp. 1851–1863.

[4] P.C. Wayner Jr., Y.K. Kao and L.V. LaCroix, The interline heat transfer coefficient of an evaporating wetting film, Int. J. Heat Mass Transfer 19 (1976), pp. 487–492.

[5] J.A. Schonberg, P.C. Wayner Jr., Analytical solution for the integral contact line evaporation heat sink, in: Proceedings of the AIAA/ASME 5th Joint Thermophysics and Heat Transfer Conference, Seattle, AIAA-1990-1787, 1990.

[6] K.P. Hallinan, H.C. Chebaro, S.J. Kim and W.S. Chang, Evaporation from an extended meniscus for nonisothermal interfacial conditions, J. Thermophys. Heat Transfer 8 (1994), pp. 709–716.

[7] S. DasGupta, J.A. Schonberg and P.C. Wayner Jr., Investigation of an evaporating extended meniscus based on the augmented Young–Laplace Equation, J. Heat Mass Transfer 115 (1993), pp. 201–208.

[8] K. Park, K. Noh and K. Lee, Transport phenomena in the thin-film region of a micro-channel, Int. J. Heat Mass Transfer 46 (2003), pp. 2381–2388.

[9] S.K. Wee, Microscale Observables for Heat and Mass Transport, Ph.D. Thesis, Texas A&M University, 2004.

[10] S. Wee, K.D. Kihm, D.M. Pratt and J.S. Allen, Microscale heat and mass transport of evaporating thin film of binary mixture, J. Thermophys. Heat Transfer 20 (2006), pp. 320–327.

[11] J.B. Freund, The atomic detail of an evaporating meniscus, Phys. Fluids 17 (2005), p. 022104.

[12] P.C. Stephan and C.A. Busse, Analysis of the heat transfer coefficient of grooved heat pipe evaporator walls, Int. J. Heat Mass Transfer 35 (1992), pp. 383–391.

[13] X. Xu and V.P. Carey, Film evaporation from a micro-grooved surface – an approximate heat transfer model and its comparison with experimental data, J. Thermophys. Heat Transfer 4 (1990), pp. 512–520

[14] H.B. Ma and G.P. Peterson, Temperature variation and heat transfer in triangular grooves with an evaporating film, J. Thermophys. Heat Transfer 11 (1997), pp. 90–97.

[15] S.J.S. Morris, The evaporating meniscus in a channel, J. Fluid Mech. 494 (2003), pp. 297–317.

[16] S. Chakraborty and S.K. Som, Heat transfer in an evaporating thin liquid film moving slowly along the walls of an inclined microchannel, Int. J. Heat Mass Transfer 48 (2005), pp. 2801–2805.

[17] R.W. Schrage, A Theoretical Study of Interface Mass Transfer, Columbia University Press, New York (1953).

[18] D.J.E. Harvie and D.F. Fletcher, A simple kinetic theory treatment of volatile liquid–gas interfaces, J. Heat Transfer 123 (2001), pp. 487–491.

[19] A. Faghri, Heat Pipe Science and Technology, Taylor & Francis, Washington, DC (1995).

[20] B. Paul, Complication of evaporation coefficients, Am. Rocket Soc. *J.* 32 (1962), pp. 1321–1328.

[21] A. Oron, S.H. Davis and S.G. Bankoff, Rev. Mod. Phys. 69 (1997), pp. 931–980.

[22] H.J. Palmer, J. Fluid Mech. 75 (1976), pp. 487–511

[23] J.P. Burelbach, S.G. Bankoff and S.H. Davis, J. Fluid Mech. 195 (1988), pp. 463–494.

[24] P.Y. WU, W.A. Little, Measurement of friction factor for flow of gases in very fine channels used for microminiature Joule–Thompson refrigerators, Cryogenics 24 (8) (1983) 273–277.

[25] X.F. Peng, G.P. Peterson, B.X. Wang, Friction flow characteristics of water flowing through rectangular microchannels, Exp. Heat Transfer 7 (1994) 249–264.

[26] J. Pfahler, J. Harlay, H. Bau, et al., Liquid and gas transport in small channels, microstructure, sensors and

actuators, ASME DSC 19 (1990) 149–157.

[27] J. Pfahler, J. Harlay, H. Bau, et al., Gas and liquid flow in small channels, micromechanical sensors, actuators and system, ASME DSC 32 (1991) 49–60.

[28] Gh. Mohiuddin Mala, D. Li, Flow characteristics of water in microtubes, Int. J. Heat Fluid Flow 20 (2) (1999) 142–148.

[29] R.S. Stanley, Two-phase flow in microchannels, Ph.D. Thesis, Louisiana Technological University, 1997. Table 3 1906 W.-h. Yang et al. / Applied Thermal Engineering 25 (2005) 1894–1907

[30] B. Xu, K.T. Ooi, N.T. Wong, Experimental investigation of flow friction for liquid flow in microchannels, Int. Commun. Heat Mass Transfer 27 (8) (2000) 1165–1176.

[31] W.M. Kays, A. London, Compact Heat Exchangers, third ed., McGraw-Hill, New York, 1984.

[32] S.-z. Hua, X.-n. Yang, Actual Fluid Friction Manual, National Defence Industry Press, Beijing, 1985, p. 269.

[33] C.L. Merkle, T. Kubota, D.R.S. Ko, An analytical study of the effects surface roughness on boundary-layer transient, AF Office of Scien. Res. Space and Missile Sys. Org., AD/A004786.

[34] J.P. Holman, Experimental Methods for Engineerings, fourth ed., McGraw-Hill, New York, 1984.

[35] Lecture notes – Department of micro and nano-technology, Technical University of Denmark.

✻✻✻✻✻